Received February 17, 2017, accepted April 6, 2017, date of publication April 12, 2017, date of current version June 7, 2017.

Digital Object Identifier 10.1109/ACCESS.2017.2693030

Minimizing Carbon Dioxide Emissions Due to Container Handling at Marine Container Terminals via Hybrid Evolutionary Algorithms

MAXIM A. DULEBENETS[1], REN MOSES[1], EREN E. OZGUVEN[1], AND ARDA VANLI[2]

[1]Department of Civil and Environmental Engineering, Florida A&M University-Florida State University, Tallahassee, FL 32310-6046 USA

[2]Department of Industrial and Manufacturing Engineering, Florida A&M University-Florida State University, Tallahassee, FL 32310-6046 USA

Corresponding author: Maxim A. Dulebenets (mdulebenets@fsu.edu)

ABSTRACT Considering a rapidly increasing seaborne trade and drastic climate changes due to emissions, produced by oceangoing vessels and container handling equipment, marine container terminal operators not only have to improve effectiveness of their operations to serve the increasing demand, but also to account for the environmental impact associated with the terminal operations. This paper proposes a novel mixed integer mathematical model for the berth scheduling problem, which minimizes the total service cost of vessels, including the total carbon dioxide emission cost due to container handling. The latter pollutant is a primary greenhouse gas that causes global warming. A Hybrid Evolutionary Algorithm, which deploys a set of local search heuristics, is developed to solve the problem. Computational experiments showcase that the optimality gap of the proposed solution algorithm does not exceed 1.61%. It is further shown that the application of additional local search heuristics allows efficient discovery of promising solutions throughout the search process. Results from numerical experiments also indicate that changes in the carbon dioxide emission cost may significantly affect the design of berth schedules. The developed mathematical model and the proposed solution algorithm can thus be adopted as effective planning tools by the marine container terminal operators and improve the environmental sustainability of the terminal operations.

INDEX TERMS Marine container terminals, carbon dioxide emissions, vessel service cost, evolutionary computation, hybrid algorithms.

I. INTRODUCTION

The international seaborne trade plays a critical role for the global economy. The volumes of the international seaborne trade have been constantly growing since 2009 and reached approximately 10.05 billion tons in 2015, which is a 27.9% increase as compared to the 2009 international seaborne trade volumes [1]. Considering such a rapid growth of the seaborne trade, marine container terminal (MCT) operators must focus on optimizing their operations [2]–[6] in order to meet the growing demand and provide timely service of the arriving vessels. The sequence of operations for handling import containers at the MCT can be described as follows. The import containers are delivered to the MCT by vessels. Once a given vessel is moored, the on-shore quay cranes start unloading the import containers. Then, those containers are placed on the internal transport vehicles (e.g., yard trucks, automated guided vehicles, straddle carries, etc.), which further transfer the containers to the dedicated area of the marshaling yard. Once the import containers are delivered by the internal transport vehicles to the assigned yard blocks of the marshaling yard, the gantry cranes unload the containers. The drayage trucks, entering the MCT via the dedicated gate, pick up the import containers and deliver them to the customers. A reverse sequence of operations is applicable for handling the export containers.

Enhancing the terminal operations is one of the primary goals for the MCT operators, but it cannot be achieved at the expense of the environment. Some of the studies, conducted to date, not only focused on improving effectiveness of the MCT operations to meet the growing demand, but also accounted for the negative environmental externalities due to container transport and handling. Golias *et al.* [7] proposed a berth scheduling policy, aiming to minimize the total late departure of vessels and indirectly decrease the fuel consumption (and hence the associated emissions) by vessels in the idle mode. Alvarez *et al.* [8] presented a

2169-3536 © 2017 IEEE. Translations and content mining are permitted for academic research only.
Personal use is also permitted, but republication/redistribution requires IEEE permission.
See http://www.ieee.org/publications_standards/publications/rights/index.html for more information.

hybrid simulation-optimization approach for assessing potential advantages from the new berth scheduling policies and liner shipping contracts, taking into consideration the fuel consumption by vessels arriving at the MCT. Esmer *et al.* [9] developed a simulation model for the Turkish MCT, aiming to reduce the environmental damage due to container handling operations. Golias *et al.* [10] formulated the berth scheduling problem (BSP), which minimized not only the total service time and delayed departures of vessels, but also the total fuel consumption and emissions, produced by vessels when sailing to the next port of call. Lang and Veenstra [11] presented a simulation-based optimization model to schedule vessel arrivals at the MCT, aiming to reduce the total fuel consumption of approaching vessels, the total diversion cost for non-handling containers, and the total vessel late departure cost. Du *et al.* [12] presented a bi-objective BSP, where the first objective minimized the total vessel late departures, while the second one aimed to minimize the total fuel consumption by vessels that were sailing to a given port of call. Wang *et al.* [13] developed an alternative solution approach to the problem, studied by Du *et al.* [12], where the static quadratic outer approximation method was used instead of the mixed integer second order cone programming model. Chen *et al.* [14] presented a methodology for improving the gate operations at the MCT, aiming to reduce the waiting time of drayage trucks and emissions produced by idling truck engines.

Several papers developed models to decrease the energy consumption by the MCT handling equipment, which could be further extended towards the reduction of emissions produced. Chang *et al.* [15] proposed an integrated berth allocation and quay crane scheduling model, aiming to minimize the total deviation between the actual and desired berthing positions, the total vessel late departure penalty, and the total energy consumption by quay cranes. He *et al.* [16] formulated a bi-objective model for scheduling yard trucks, shared among multiple MCTs, where the first objective aimed to minimize the total overflowed workloads, while the second one minimized the total yard truck energy consumption. He *et al.* [17] proposed a yard crane scheduling model, where the first objective minimized the total task completion delay, while the second one aimed to minimize the total energy consumption associated with completion of all the tasks. He *et al.* [18] presented a mathematical formulation for the integrated internal truck, yard crane, and quay crane scheduling problem. The first objective aimed to minimize the total delayed vessel departures, while the second one minimized the total transportation energy consumption.

This study focuses on modeling the BSP, which aims to identify the assignment of arriving vessels to the MCT berthing positions and determine the sequence of vessels that will be served at each berthing position. The review of the MCT literature shows that some of the BSP models, developed in the past, captured the emission production by the arriving vessels; however, none of the models directly accounted for the emission production due to container handing in berth scheduling. To fill the latter gap in the state-of-the-art this study proposes a novel mixed integer BSP model, which minimizes the total vessel service cost, including the carbon dioxide (CO_2) emission cost due to container handling. A Hybrid Evolutionary Algorithm, which applies a set of local search heuristics, is developed to solve the proposed mathematical model. Reduction of CO_2 emissions throughout the container handling process is crucial, as CO_2 is a primary greenhouse gas that causes global warming [19]. The latter concern is considered as of a high importance, taking into account the existing predictions of the average global temperatures to rise by up to 5.8 °C by the year of 2100 [20]. The remainder of the paper is organized in the following order. Section II provides a detailed problem description, while Section III presents the mathematical formulation. Section IV discusses the main features of the proposed solution approach, while Section V presents a set of numerical experiments that were performed in order to assess effectiveness of the developed solution approach and the berth scheduling model. The last section discusses the main findings and outlines the future research avenues.

II. PROBLEM DESCRIPTION

This paper studies the BSP at a typical MCT that has a discrete berth layout, where the MCT wharf is divided into a set of berths. Only one vessel can be handled at each berth at the time. The latter MCT configuration has been widely used in the berth scheduling literature published to date [21], [22]. Let $V = \{1, \ldots, m\}$ be a set of vessels, which request service at the MCT, and $B = \{1, \ldots, n\}$ be a set of available MCT berths. The dynamic case is adopted in this study for vessel arrivals, where the MCT operator has the information regarding the expected arrival time for each vessel. It is assumed that the arrival times of vessels are deterministic; therefore, the uncertainty that may be caused by changes in the weather conditions, unexpected delays in service at the preceding ports of call, alterations in vessel schedules, and other factors is not captured in this study. The vessels, arriving for service at the MCT, are towed by push boats to their assigned berths. If a given vessel arrives at the port, but the assigned berth is not available (e.g., the berth is being occupied by another vessel), the push boats will tow that vessel to a dedicated waiting area (Fig. 1). This study assumes that a waiting cost c_v^{WT}, $v \in V$ (USD per hour) will be imposed to the MCT operator. The latter assumption can be justified by the fact that an increasing number of vessels in the waiting area may result in congestion at the MCT seaside, which shall further cause delays for vessels that enter and leave the MCT.

Loading and unloading of containers at each MCT berth is performed by the quay cranes. This study assumes that safety distances between vessels, served at the MCT berths, and safety distances between the quay cranes are maintained. The liner shipping companies have contractual agreements with the MCT operator, according to which the MCT operator is able to provide a set of handling rates $H = \{1, \ldots, k\}$

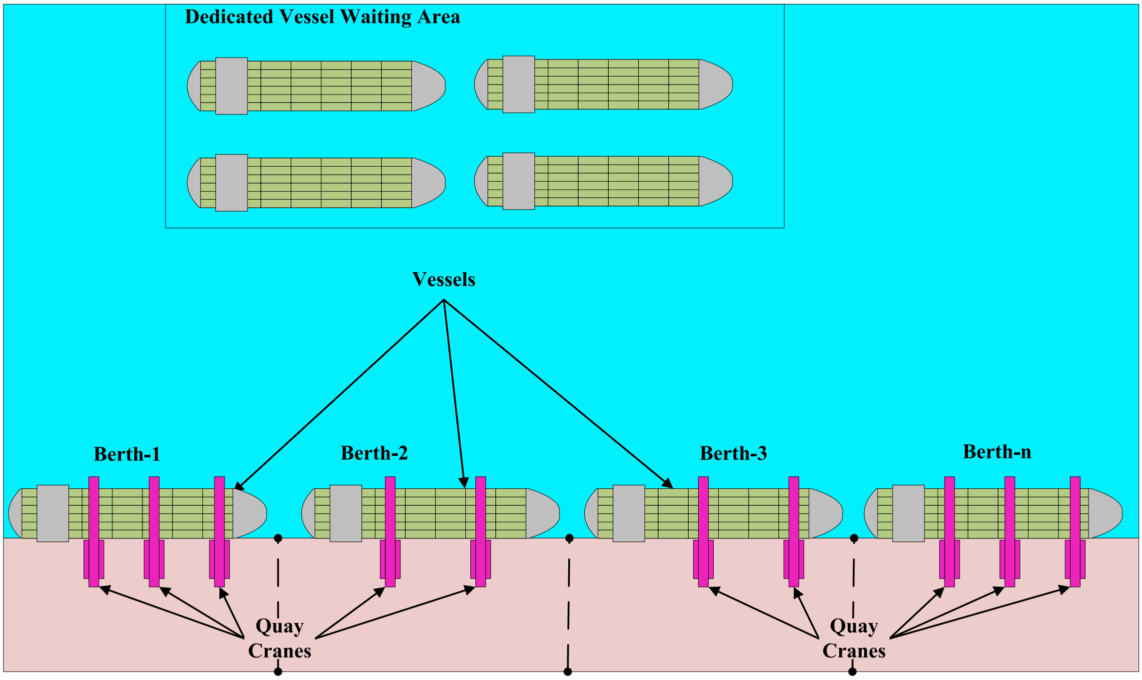

FIGURE 1. Seaside operations at the MCT.

for the vessel service. A handling productivity hp_{vbh}, $v \in V$, $b \in B$, $h \in H$, generally estimated in twenty-foot equivalent units (TEUs) per hour, is associated with each handling rate. A handling cost c_{vh}^{HT}, $v \in V$, $h \in H$ (USD per TEU) for serving a given vessel is assumed to increase, if a handling rate with a higher productivity is requested. Furthermore, selection of handling rates with higher handling productivities by the liner shipping companies will require the MCT operator to deploy more handling equipment for service of vessels, which will increase the total amount of emissions produced due to container handling. This study models production of the CO_2 emissions, which are computed based on the total amount of containers to be handled NC_v, $v \in V$ (TEUs) and the associated CO_2 emission factor EF_{vbh}, $v \in V$, $b \in B$, $h \in H$ (tons of CO_2 per TEU). The latter methodology was adopted based on the available literature [23], [24].

The MCT operator has to perform a preliminary allocation of vessels to berths, scheduling of handling resources, and assignment of containers to specific storage areas based on the expected vessel arrival times and the handling rates, negotiated with the liner shipping companies. If due to changes in the preliminary berth schedule a vessel is diverted from its originally assigned berth (i.e., "*preferred berth*") for service at another berth, the handling productivity for the requested handling rate is assumed to decrease. The latter assumption can be supported by the fact that the distance, traveled by the internal transport vehicles to the dedicated storage area from the other MCT berths, is generally larger than the travel distance from the "*preferred berth*". The vessel handling time $\boldsymbol{HT}_v$, $v \in V$ (hours) is calculated based on the actual handling productivity and the total amount of containers to be handled for that vessel. The vessel handling time uncertainty (which may be caused by changes in scheduling of the internal transport vehicles, breakdowns in handling equipment, terminal congestion, etc.) is not captured in this paper.

The liner shipping companies have to account for the vessel handling time at ports of call in design of their schedules [22]. This study assumes that the requested departure time RD_v, $v \in V$ (hours) is negotiated between a given liner shipping company and the MCT operator for each vessel. A vessel late departure penalty c_v^{LD}, $v \in V$ (USD per hour) will be incurred by the MCT operator for violation of the requested vessel departure times. The main objective of the BSP studied herein is to design a cost-effective berth schedule, which will minimize the total service cost of vessels calling at the MCT, including the total vessel handling cost, the total waiting cost, the total vessel late departure penalty, and the total CO_2 emission cost.

III. MATHEMATICAL MODEL

This section defines the notations that will be further used throughout the paper and presents a mixed integer mathematical model for the discrete dynamic green berth scheduling problem (**GBSP**).

A. NOTATIONS

Sets:

$V = \{1, \ldots, m\}$	set of vessels to be served at the MCT
$B = \{1, \ldots, n\}$	set of berths available at the MCT
$H = \{1, \ldots, k\}$	set of handling rates available at the MCT

Decision Variables:

$\boldsymbol{x}_{vb}, v \in V, b \in B$	=1 if vessel v is assigned for service at berth b (=0 otherwise)
$\boldsymbol{s}_{\underline{v}\overline{v}}, \underline{v}, \overline{v} \in V, \underline{v} \neq \overline{v}$	=1 if vessel $\overline{v}$ is assigned for service at the same berth immediately after vessel $\underline{v}$ (=0 otherwise)
$\boldsymbol{f}_v, v \in V$	=1 if vessel v is served as the first vessel at the given berth (=0 otherwise)
$\boldsymbol{l}_v, v \in V$	=1 if vessel v is served as the last vessel at the given berth (=0 otherwise)
$\boldsymbol{z}_{vbh}, v \in V, b \in B, h \in H$	=1 if handling rate h is selected for service of vessel v at berth b (=0 otherwise)

Auxiliary Variables:

$\boldsymbol{ST}_v, v \in V$	start time of service for vessel v (hours)
$\boldsymbol{HT}_v, v \in V$	handling time of vessel v (hours)
$\boldsymbol{WT}_v, v \in V$	waiting time of vessel v (hours)
$\boldsymbol{LD}_v, v \in V$	hours of late departure for vessel v (hours)
$\boldsymbol{CO_2}_v, v \in V$	total amount of CO_2 emissions produced from serving vessel v (tons)

Parameters:

$AT_v, v \in V$	expected arrival time of vessel v (hours)
$NC_v, v \in V$	number of containers to be handled for vessel v (TEUs)
$hp_{vbh}, v \in V, b \in B, h \in H$	handling productivity for vessel v at berth b under handling rate h (TEUs/hour)
$RD_v, v \in V$	requested departure time for vessel v (hours)
$EF_{vbh}, v \in V, b \in B, h \in H$	CO_2 emission factor for vessel v served at berth b under handling rate h (tons of CO_2/TEU)
$c_{vh}^{HT}, v \in V, h \in H$	handling cost for vessel v under handling rate h (USD/TEU)
$c_v^{WT}, v \in V$	waiting cost for vessel v (USD/hour)
$c_v^{LD}, v \in V$	penalty for late departure of vessel v (USD/hour)
c^{CO_2}	CO_2 emission cost (USD/ton)
M	large positive number

B. MIXED INTEGER MATHEMATICAL MODEL

The discrete dynamic green berth scheduling problem (**GBSP**) can be formulated as a mixed integer programming model as follows.

GBSP: Green Berth Scheduling Problem

$$\min\Big[\sum_{v\in V}\sum_{b\in B}\sum_{h\in H}(NC_v c_{vh}^{HT} \boldsymbol{z}_{vbh}) + \sum_{v\in V}(\boldsymbol{WT}_v c_v^{WT}) + \sum_{v\in V}(\boldsymbol{LD}_v c_v^{LD}) + \sum_{v\in V}(\boldsymbol{CO_2}_v c^{CO_2})\Big] \tag{1}$$

Subject to:

$$\sum_{b\in B}\boldsymbol{x}_{vb} = 1 \forall v \in V \tag{2}$$

$$\sum_{b\in B}\sum_{h\in H}\boldsymbol{z}_{vbh} = 1 \forall v \in V \tag{3}$$

$$\boldsymbol{z}_{vbh} \leq \boldsymbol{x}_{vb} \forall v \in V, b \in B, h \in H \tag{4}$$

$$\boldsymbol{f}_{\overline{v}} + \sum_{\underline{v}\in V \neq \overline{v}}\boldsymbol{s}_{\underline{v}\overline{v}} = 1 \forall \overline{v} \in V \tag{5}$$

$$\boldsymbol{l}_{\underline{v}} + \sum_{\overline{v}\in V \neq \underline{v}}\boldsymbol{s}_{\underline{v}\overline{v}} = 1 \forall \underline{v} \in V \tag{6}$$

$$\boldsymbol{f}_{\underline{v}} + \boldsymbol{f}_{\overline{v}} \leq 3 - \boldsymbol{x}_{\underline{v}b} - \boldsymbol{x}_{\overline{v}b} \forall \underline{v}, \overline{v} \in V, \underline{v} \neq \overline{v}, b \in B \tag{7}$$

$$\boldsymbol{l}_{\underline{v}} + \boldsymbol{l}_{\overline{v}} \leq 3 - \boldsymbol{x}_{\underline{v}b} - \boldsymbol{x}_{\overline{v}b} \forall \underline{v}, \overline{v} \in V, \underline{v} \neq \overline{v}, b \in B \tag{8}$$

$$\boldsymbol{s}_{\underline{v}\overline{v}} - 1 \leq \boldsymbol{x}_{\underline{v}b} - \boldsymbol{x}_{\overline{v}b} \leq 1 - \boldsymbol{s}_{\underline{v}\overline{v}} \forall \underline{v}, \overline{v} \in V, \underline{v} \neq \overline{v}, b \in B \tag{9}$$

$$\boldsymbol{ST}_v \geq AT_v \forall v \in V \tag{10}$$

$$\boldsymbol{HT}_v = \sum_{b\in B}\sum_{h\in H}\Big(\frac{NC_v}{hp_{vbh}}\Big)\boldsymbol{z}_{vbh} \forall v \in V \tag{11}$$

$$\boldsymbol{ST}_{\overline{v}} \geq \boldsymbol{ST}_{\underline{v}} + \boldsymbol{HT}_{\underline{v}} - M(1 - \boldsymbol{s}_{\underline{v}\overline{v}}) \forall \underline{v}, \overline{v} \in V, \underline{v} \neq \overline{v} \tag{12}$$

$$\boldsymbol{WT}_v \geq \boldsymbol{ST}_v - AT_v \forall v \in V \tag{13}$$

$$\boldsymbol{LD}_v \geq \boldsymbol{ST}_v + \boldsymbol{HT}_v - AT_v \forall v \in V \tag{14}$$

$$\boldsymbol{CO_2}_v = NC_v \sum_{b\in B}\sum_{h\in H} EF_{vbh}\boldsymbol{z}_{vbh} \forall v \in V \tag{15}$$

$$\boldsymbol{x}_{vb}, \boldsymbol{s}_{\underline{v}\overline{v}}, \boldsymbol{f}_v, \boldsymbol{l}_v, \boldsymbol{z}_{vbh} \in \{0, 1\} \forall \underline{v}, \overline{v} \in V, \underline{v} \neq \overline{v}, b \in B, h \in H \tag{16}$$

$$NC_v \in N \tag{17}$$

$$\boldsymbol{ST}_v, \boldsymbol{HT}_v, \boldsymbol{WT}_v, \boldsymbol{LD}_v, \boldsymbol{CO_2}_v, AT_v, hp_{vbh}, RD_v, EF_{vbh}, c_{vh}^{HT}, c_v^{WT}, c_v^{LD}, c^{CO_2}, M \in R^+ \forall v \in V, b \in B, h \in H \tag{18}$$

In **GBSP** the objective function minimizes the total vessel service cost, which includes the following components: (a) the total vessel handling cost; (b) the total vessel waiting cost; (c) the total vessel late departure cost; and (d) the total CO_2 emission cost due to container handling. Constraints set (2) guarantees that each vessel, arriving at the MCT, should be served at one of the MCT berths. Constraints set (3) ensures that one handling rate should be selected by the MCT operator for service of a given vessel. Constraints set (4) indicates that service of a vessel under the selected handling rate should be performed at the assigned MCT berth. Constraints set (5) ensures that a given vessel, calling for service at MCT, can be either served first or after the other vessel, assigned to the same MCT berth. Constraints set (6) indicates that a given vessel, calling for service at MCT, can be either served last or before the other vessel, assigned to the same MCT berth. Constraints set (7) states that only one vessel will be served first at the given MCT berth. Constraints set (8) guarantees that only one vessel will be served last at the given MCT berth. Constraints set (9) states that a given vessel may be served after another vessel only if both vessels are scheduled for service at the same MCT berth. Constraints set (10) indicates the service of each vessel can begin only after its arrival at the MCT. Constraints set (11) computes the handing time of each vessel at the assigned MCT berth under the selected handling rate. Constraints set (12) calculates the start time of service for each one of the vessels to be served at the MCT. Constraints set (13) computes the waiting time for each one of the vessels to be served at the MCT. Constraints set (14) estimates the hours of late departure for each one of the vessels to be served at the MCT. Constraints set (15) computes the total amount of CO_2 emissions produced as a result of serving a given vessel due to container handling. Constraints sets (16)-(18) show the nature of all parameters and variables of the **GBSP** mathematical model.

IV. SOLUTION APPROACH

The **GBSP** mathematical model may be reduced to the unrelated machine scheduling problem [25]. The machine scheduling problems have the *NP*-hard complexity; therefore, the exact optimization algorithms will not be able to obtain solutions for the realistic size problem instances of the **GBSP** mathematical model within a reasonable computational time. To address the latter drawback this study proposes a Hybrid Evolutionary Algortihm (HEA) for solving the **GBSP** mathematical model. As opposed to canonical EAs, which primarily apply stochastic search operators without considering any feedback from the search and performing any local search within the promising domains, the proposed HEA deploys two types of local search heuristics. The first local search heuristic is applied at the population initialization stage, while the second one is executed after performing the HEA operations (i.e., crossover and mutation). Hybridization of the algorithms via deployment of local search heuristics generally allows more efficient exploration and exploitation of the problem search space, enhancing the objective function values at termination of the algorithm, and improving the algorithmic convergence patterns [26]. The major steps of the proposed HEA are shown in Fig. 2.

The required data structures for the HEA variables are initialized in step 0. Next, the HEA algorithm generates the chromosomes for the initial population using a local search heuristic in step 1. The fitness function values are computed for each one of chromosomes of the initial population in step 2. Then, the HEA algorithm begins an iterative process, where the parent chromosomes are selected in step 3. The offspring chromosomes are produced via the HEA operations in step 4. Furthermore, in step 4 the HEA algorithm deploys a custom operator to repair the infeasible offspring, generated as a result of the HEA operations, and a local search heuristic to improve fitness of the offspring chromosomes. Next,

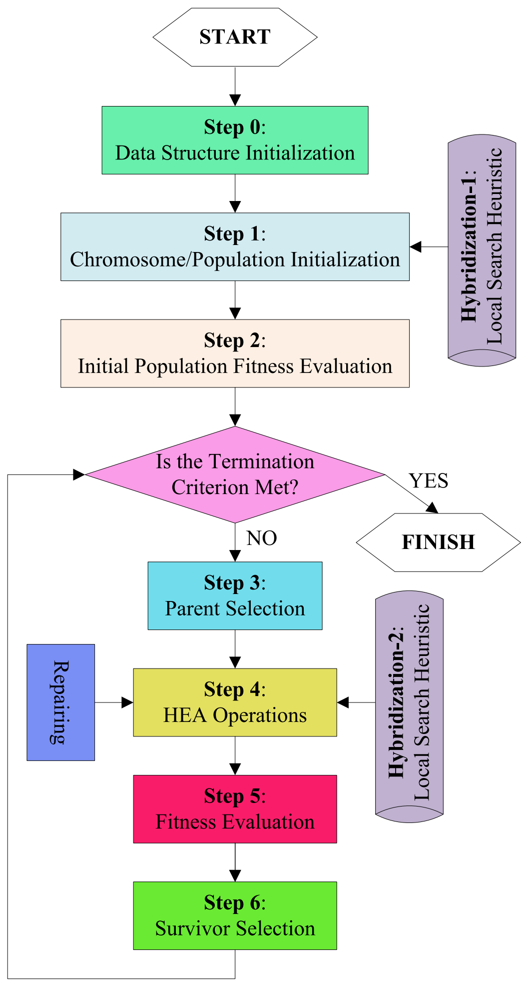

FIGURE 2. The main steps of the HEA algorithm.

the fitness function values are calculated for the offspring chromosomes in step 5. The survivor selection procedure is performed in step 6. The iterative process is stopped by the HEA algorithm, when the termination criterion is achieved. At termination the HEA algorithm returns the best discovered solution, which represents the vessel to berth to handling rate assignment with the lowest possible vessel service cost. A comprehensive description of each algorithmic step is provided next.

A. REPRESENTATION OF CHROMOSOMES

This study uses a three-dimensional integer chromosome to represent the vessel to berth to handling rate assignment (i.e., solution for the **GBSP** mathematical model). Fig. 3 demonstrates an example of a chromosome, where we observe that 9 vessels request service at the MCT, which has 2 berths. Vessels "2", "4", "5", "7", and "9" are scheduled for service at berth "1" of the MCT (in that specific service order) under handling rates "2", "2", "1", "1", and "4" respectively, while vessels "1", "3", "6", and "8" are scheduled for service at berth "2" of the MCT (in that specific service order) under handling

Berth →	1	1	1	1	1	2	2	2	2
Vessel →	2	4	5	7	9	1	3	6	8
Handling Rate →	2	2	1	1	4	3	3	1	2

FIGURE 3. An example of a chromosome.

rates "3", "3", "1", and "2" respectively. Each chromosome is composed of gene arrays. Specifically, each gene array includes three genes, representing berth, vessel, and handling rate. Note that the length of a chromosome remains the same throughout evolution of the HEA algorithm and is defined by the number of vessels calling for service at the MCT (i.e., $|V|$).

B. INITIALIZATION OF CHROMOSOMES AND POPULATION

Canonical EAs primarily rely on chromosomes and initial populations that are generated randomly [26]. Stochastic chromosome initialization operators allow maintaining diversity of the initial population, but in the meantime may generate infeasible and low quality individuals. To avoid the latter shortcoming, the proposed HEA algorithm relies on a local search heuristic for the chromosome initialization, which is based on the Green First Come First Served Policy (GFCFS). The GFCFS heuristic is an extension of the FCFS policy, which has been widely used in the BSP literature [22], [27]. Unlike a typical FCFS heuristic, the GFCFS policy makes an assumption regarding the handling rate, selected by the MCT operator for service of the arriving vessels. Specifically, the GFCFS heuristic choses the handling rate with the lowest productivity for each vessel, calling for service at the MCT, to reduce production of CO_2 emissions due to container handling. Let V^S be a set of vessels that are sorted based on their arrival times; $\boldsymbol{BA}_b$ be the time when berth b is idle for the first time in the given planning horizon; and $\boldsymbol{FT}_v$ be the finish service time of vessel v. The major steps of the GFCFS heuristic are demonstrated in Pseudocode 1 (**P-1**).

The necessary data structures are generated in step 1. Then, all vessels that call for service at the MCT are sorted based on their times of arrival in the ascending order in step 2. Next, GFCFS starts an iterative process (steps 4-13). GFCFS identifies the first available berth in step 5. The handling rate with the lowest handling productivity is selected in step 6. Then, GFCFS assigns a vessel to the first available berth for service under the selected handling rate in step 7. The start service time for a vessel is estimated in step 8, while the vessel handling time is computed in step 9. The finish time of a vessel service is calculated in step 10, while the procedure updates the berth availability in step 11. The GFCFS heuristic stops the iterative process, once the initial vessel to berth to handling rate assignment is determined.

The advantage of using GFCFS for the chromosome and population initialization within the proposed HEA is that it will guarantee feasibility and acceptable quality of the individuals. However, GFCFS is deterministic. The population, initialized using GFCFS only, will have identical individuals, which will negatively affect the population diversity.

P-1 Green First Come First Served Policy (GFCFS)

GFCFS$(V, B, H, AT_v, NC_v, hp_{vbh})$
in: $V = \{1, \ldots, m\}$- set of vessels; $B = \{1, \ldots, n\}$- set of berths; $H = \{1, \ldots, k\}$- set of handling rates; AT_v- arrival time of vessel v; NC_v- number of containers to be handled for vessel v; hp_{vbh}- handling productivity of vessel v at berth b under handling rate h
out: z_{vbh}- vessel to berth to handling rate assignment
1: $|V^S| \leftarrow m$; $|\boldsymbol{BA}| \leftarrow n$; $|z_{vbh}| \leftarrow n \cdot m \cdot k$; $|\boldsymbol{ST}| \leftarrow m$; $|\boldsymbol{FT}| \leftarrow m$
2: $V^S \leftarrow$ ***Sort***(V, AT)
3: $v \leftarrow 1$
4: **for all** $v \in V^S$ **do**
5: $\quad b \leftarrow \arg\min_b(\boldsymbol{BA}_b)$
6: $\quad h \leftarrow \arg\min_h(hp_{vbh})$
7: $\quad z_{vbh} \leftarrow 1$
8: $\quad \boldsymbol{ST}_v \leftarrow \max(AT_v, \boldsymbol{BA}_b)$
9: $\quad \boldsymbol{HT}_v \leftarrow \sum_{b \in B} \sum_{h \in H} \left(\frac{NC_v}{hp_{vbh}}\right) z_{vbh}$
10: $\quad \boldsymbol{FT}_v \leftarrow \boldsymbol{ST}_v + \boldsymbol{HT}_v$
11: $\quad \boldsymbol{BA}_b \leftarrow \boldsymbol{FT}_v$
12: $\quad v \leftarrow v + 1$
13: **end for**
14: **return** z_{vbh}

To ensure diversity of the initial population half of the HEA population will be initialized using GFCFS, while the rest of the HEA population will be initialized randomly. The HEA population size (*PopSize*) will be determined as a result of the parameter tuning analysis (details are presented in section V.B of the paper). Size of the population is assumed to remain fixed throughout the HEA evolution.

C. PARENT SELECTION

The parent selection step plays an important role in the EA evolution, as it determines a subset of individuals from the population that will be able to participate in the EA operations and produce the offspring chromosomes. The proposed HEA deploys the roulette wheel selection (which is also known as a fitness proportionate selection) mechanism for the identification of parent chromosomes, which is widely used in canonical Genetic Algorithms [26]. The roulette wheel selection is a stochastic selection procedure, which assumes that a probability of a given individual to become a parent is proportional to its fitness. For a detailed description of the roulette wheel selection mechanism this study refers to Eiben and Simth [26].

D. HEA OPERATIONS

Once the parent chromosomes are identified, the HEA algorithm applies three operators to produce the offspring at a given generation, including the following: 1) crossover operator; 2) mutation operator; and 3) hybrid operator. A detailed description of those operators is provided in sections IV.D.1- IV.D.3 of the paper.

1) CROSSOVER

For the chromosome representation, adopted in this study (Fig. 3), typical crossover operators (e.g., one-point crossover, uniform crossover, multi-point crossover, etc.) may generate the infeasible offspring, where vessels will be assigned for service several times. However, there are certain special crossover operators (e.g., order crossover, partially mapped crossover), which will be able to produce the feasible offspring for the adopted type of chromosomes. The proposed HEA deploys the order crossover operator. An example of the crossover operation is illustrated in Fig. 4.

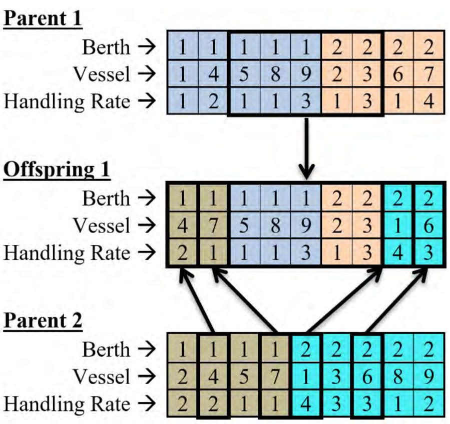

FIGURE 4. An example of a crossover operation.

In the provided example two parent chromosomes are randomly selected from the population. Then, a segment of the chromosome (the segment length is determined randomly) from the first parent is copied to the first offspring chromosome. In the considered example arrays of genes with vessels "5", "8", "9", "2", and "3" are copied from the first parent to the first offspring chromosome. Next, the order crossover operator selects the gene arrays with missing vessels from the second parent and copies them to the first offspring chromosome. In the considered example arrays of genes with vessels "4", "7", "1", and "6" are copied from the second parent to the first offspring chromosome. The second offspring is created in a similar fashion.

The probability of randomly selected parent chromosomes to undergo a crossover operation is defined by parameter *CrosProb*. The *CrosProb* value will be set as a result of the parameter tuning analysis (details are presented in section V.B of the paper). Note that the mutation operation will be still performed for a pair of parent chromosomes that do not undergo the crossover operation.

2) MUTATION

After application of the order crossover operator the developed HEA deploys a custom mutation operator. A large variety of mutation operators have been implemented in EAs, including bit flipping, floating point, scramble, insert, invert, swap, etc. [26]. Many BSP studies rely on the swap mutation due to its effectiveness [7], [10]. However, for the proposed chromosome representation the swap mutation will be effective for altering the genes with vessel values, but may cause shortcomings when changing the genes with berth and handling rate values. Specifically, by swapping genes with berth or handling rate values, the swap mutation operator will not be able to discover any other potential values for the berth or handling rate. For instance, if vessels "1" and "2" are served under handling rates "3" and "4" respectively, the swap mutation operator will assign handling rate "4" for vessel "1", while handling rate "3" will be assigned for vessel "2". Hence, the other handling rate alternatives (e.g., handling rates "1", "2", etc.) will never be considered.

The latter drawback can be addressed by applying the floating point mutation operator for altering the genes with berth and handling rate values, which changes berth and handling rate values based on pre-specified lower and upper bounds (and rounds the generated random value to the nearest integer). The custom mutation operator, developed in this study, applies the swap mutation for altering the genes with vessel values and the floating point mutation for the genes with berth and handling rate values. The main steps of the mutation operation procedure are demonstrated in Pseudocode 2 (**P-2**).

The data structure for the mutated offspring is initialized in step 1. Then, the procedure enters the loop (steps 3-17), where for each offspring chromosome function ***GenerRandVal*** generates a random integer value, ranging from "1" to "3". Next, if the generated random value is equal to "1", the mutation operator applies the floating point mutation to the genes with berth values of the offspring chromosome (step 8). If the generated random value is equal to "2", the mutation operator applies the swap mutation to the genes with vessel values of the offspring chromosome (step 10). If the generated random value is equal to "3", the mutation operator applies the floating point mutation to the genes with handling rate values of the offspring chromosome (step 12). The procedure terminates once each one of the offspring chromosomes has been mutated. The number of genes mutated for each offspring chromosome is determined by the mutation rate (*MutRate*). The *MutRate* value will be set as a result of the parameter tuning analysis (details are presented in section V.B of the paper).

An example of a mutation operation is demonstrated in Fig. 5, where we observe that vessels "9" and "1", originally scheduled at berths "1" and "2", switch their berth assignments. Furthermore, vessel "4", originally assigned for service at berth "1" is diverted for service at berth "2"; whereas vessel "8", originally assigned for service at berth "2", is diverted for service at berth "1". The handling rates for vessels "7" and "3" are updated from "1" and "3" to "2" and "4" respectively. A total of six genes have been mutated in the considered example (i.e., $MutRate = 6$).

3) HEA OPERATIONS HYBRIDIZATION

Both crossover and mutation operators are stochastic and do not consider any specific properties of the **GBSP** mathematical model. An additional operator was encoded

P-2 Mutation Operation

Mutation$(Offspring_{gen}, MutRate)$
in: $Offspring_{gen}$- offspring produced by crossover at generation gen; $MutRate$ - mutation rate
out: $\overline{Offspring_{gen}}$- mutated offspring at generation gen

$|\overline{Offspring_{gen}}| \leftarrow |Offspring_{gen}|$
$i \leftarrow 1$
for all $i \in Offspring_{gen}$ **do**
  $j \leftarrow 1$
  while $j \leq MutRate$ **do**
    $RandVal \leftarrow$ ***GenerRandVal***
    if $\overline{RandVal = 1}$ **then**
      $\overline{Offspring^{berth}_{gen_i}} \leftarrow$ ***Float***$(Offspring^{berth}_{gen_i})$
    else if $\overline{RandVal}$ $= 2$ **then**
      $\overline{Offspring^{vessel}_{gen_i}} \leftarrow$ ***Swap***$(Offspring^{vessel}_{gen_i})$
    else if $\overline{RandVal}$ $= 3$ **then**
      $\overline{Offspring^{rate}_{gen_i}} \leftarrow$ ***Float***$(Offspring^{rate}_{gen_i})$
    end if
    $j \leftarrow j + 1$
  end while
  $i \leftarrow i + 1$
end for
return $\overline{Offspring_{gen}}$

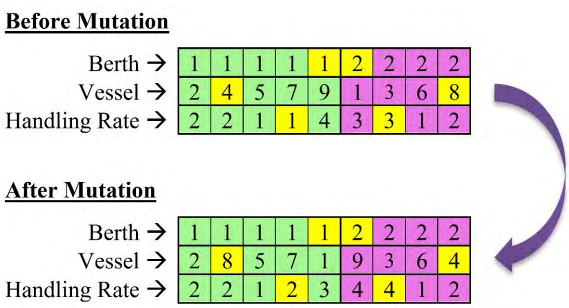

FIGURE 5. An example of a mutation operation.

within the developed HEA algorithm to refine the vessel to berth to handling rate assignment after performing crossover and mutation operations. Note that the problem of optimal vessel to berth assignment at the MCT for the offspring chromosomes, generated using crossover and mutation operators, is a typical BSP with the NP-hard complexity that will require a substantial computational time. However, selection of the optimal handling rates for service of vessels can be reduced to a typical assignment problem, which will require less computational efforts. The problem of the optimal handling rate selection for service of vessels calling at the MCT is a relaxation of the **GBSP** mathematical model (that will be referred to as **GBSP-R**) and is formulated as follows.

GBSP-R: Reduced Green Berth Scheduling Problem

$$\min\Big[\sum_{v\in V}\sum_{b\in B}\sum_{h\in H}(NC_v c^{HT}_{vh} z_{vbh}) + \sum_{v\in V}(\boldsymbol{WT}_v c^{WT}_v) + \sum_{v\in V}(\boldsymbol{LD}_v c^{LD}_v) + \sum_{v\in V}(\boldsymbol{CO_2}_v c^{CO_2})\Big] \quad (19)$$

Subject to:

$$\sum_{b\in B}\sum_{h\in H} z_{vbh} = 1 \forall v \in V \quad (20)$$

$$z_{vbh} \leq x_{vb} \forall v \in V, b \in B, h \in H \quad (21)$$

$$\boldsymbol{ST}_v \geq AT_v \forall v \in V \quad (22)$$

$$\boldsymbol{HT}_v = \sum_{b\in B}\sum_{h\in H}\Big(\frac{NC_v}{hp_{vbh}}\Big) z_{vbh} \forall v \in V \quad (23)$$

$$\boldsymbol{ST}_{\bar{v}} \geq \boldsymbol{ST}_{\underline{v}} + \boldsymbol{HT}_{\underline{v}} - M(1 - s_{\underline{v}\bar{v}}) \forall \underline{v}, \bar{v} \in V, \underline{v} \neq \bar{v} \quad (24)$$

$$\boldsymbol{WT}_v \geq \boldsymbol{ST}_v - AT_v \forall v \in V \quad (25)$$

$$\boldsymbol{LD}_v \geq \boldsymbol{ST}_v + \boldsymbol{HT}_v - AT_v \forall v \in V \quad (26)$$

$$\boldsymbol{CO_2}_v = NC_v \sum_{b\in B}\sum_{h\in H} EF_{vbh} z_{vbh} \forall v \in V \quad (27)$$

$$x_{vb}, s_{\underline{v}\bar{v}}, z_{vbh} \in \{0, 1\} \forall \underline{v}, \bar{v} \in V, \underline{v} \neq \bar{v}, b \in B, h \in H \quad (28)$$

$$NC_v \in N \quad (29)$$

$$\boldsymbol{ST}_v, \boldsymbol{HT}_v, \boldsymbol{WT}_v, \boldsymbol{LD}_v, \boldsymbol{CO_2}_v, AT_v, hp_{vbh}, RD_v, EF_{vbh}, c^{HT}_{vh}, c^{WT}_v, c^{LD}_v, c^{CO_2}, M \in R^+ \forall v \in V, b \in B, h \in H \quad (30)$$

In **GBSP-R** the objective function (19) minimizes the total vessel service cost. Constraints set (20) indicates that one handling rate should be selected for service of a given vessel. Constraints set (21) ensures that service of a vessel under the selected handling rate should be performed at the assigned MCT berth. Constraints set (22) guarantees that service of a given vessel can begin only after its arrival at the MCT. Constraints sets (23)-(27) estimate handling time, start service time, waiting time, hours of late departure, and CO_2 emission production respectively for each vessel. Constraints sets (28)-(30) show the nature of all parameters and variables of the **GBSP-R** mathematical model. Unlike the **GBSP** mathematical model, where the vessel to berth assignment and the vessel service order are determined using decision variables $\boldsymbol{x}_{vb}$, $v \in V, b \in B$ and $\boldsymbol{s}_{\underline{v}\bar{v}}, \underline{v}, \bar{v} \in V, \underline{v} \neq \bar{v}$ respectively, the **GBSP-R** mathematical model assumes that the vessel to berth assignment and the vessel service order are already known and determined by crossover and mutation operators (hence, x_{vb}, $v \in V, b \in B$ and $s_{\underline{v}\bar{v}}, \underline{v}, \bar{v} \in V, \underline{v} \neq \bar{v}$ are declared as parameters).

The **GBSP-R** mathematical model can be solved using commercial mixed integer programming optimization solvers (e.g., CPLEX) for realistic size problem instances within an acceptable computational time. However, solving **GBSP-R** for each individual in the population at each generation may negatively affect the time complexity of the HEA algorithm. To avoid an increase in the HEA time complexity the optimal handling rate for each vessel will be determined by solving the **GBSP-R** mathematical model only for a subset of individuals in the population (Ω) and after pre-specified number of generations (Gen_Ω). The local search heuristic, which determines the optimal handling rate for a randomly selected subset of the offspring chromosomes in the

HEA population after pre-specified number of generations, will be further referred to as the Optimal Handling Rate Selection (OHRS) heuristic. The main steps of the OHRS heuristic are demonstrated in Pseudocode 3 (**P-3**).

P-3 Optimal Handling Rate Selection (OHRS) Heuristic

$\boldsymbol{OHRS}(InData, Offspring_{gen}, \Omega, Gen_{\Omega})$
in: $InData$- input parameter values for the **GBSP-R** model; $Offspring_{gen}$- offspring at generation gen; Ω- subset of the offspring selected for improvement; Gen_{Ω}- number of generations after each improvement
out: $\overline{Offspring_{gen}}$- updated offspring at generation gen
1: $|\overline{Offspring_{gen}}| \leftarrow |Offspring_{gen}|$
2: $gen_{aux} \leftarrow 1$
3: **if** $gen = gen_{aux}$ **then**
4: $\quad i \leftarrow 1$
5: $\quad$ **for all** $i \in Offspring_{gen}$ **do**
6: $\quad\quad$ **if** $Offspring_{gen_i} \in \Omega$ **then**
7: $\quad\quad\quad \overline{Offspring^{rate}_{gen_i}} \leftarrow \boldsymbol{GBSP-R}(InData, Offspring^{rate}_{gen_i})$
8: $\quad\quad$ **end if**
9: $\quad\quad i \leftarrow i + 1$
10: $\quad$ **end for**
11: $\quad gen_{aux} \leftarrow gen_{aux} + Gen_{\Omega}$
12: **end if**
13: **return** $\overline{Offspring_{gen}}$

The data structure for the updated offspring is initialized in step 1, while the first generation for refining the handling rate assignment (gen_{aux}) is set to 1 in step 2. Next, if $gen = gen_{aux}$ the ORHS heuristic starts an iterative process (steps 5-10), where the optimal handling rate is determined only for a subset of the offspring individuals (Ω) by solving the **GBSP-R** mathematical model (step 7). The next generation for refining the handling rate assignment is reset in step 11. The OHRS heuristic is continuously executed every Gen_{Ω} generations within the HEA algorithm until the HEA convergence criterion is met. Values of Ω and Gen_{Ω} parameters and will be determined as a result of the parameter tuning analysis, and details will be discussed in section V.B of the paper.

E. REPAIRING INFEASIBLE INDIVIDUALS

The HEA mutation operator may produce the infeasible individuals throughout evolution of the algorithm. Fig. 6 illustrates an example of an infeasible offspring chromosome, where the service order of vessels at berth "1" is disrupted by vessels "4" and "5" that are assigned for service at berth "2".

Infeasible individuals represent erroneous solutions for the **GBSP** mathematical model and have to be altered in order to avoid the genetic drift [26] and ensure feasibility of the final solution at convergence. An additional operator was designed within the proposed HEA algorithm to repair the infeasible chromosomes. The key steps, required for the repairing operation, are demonstrated in Pseudocode 4 (**P-4**).

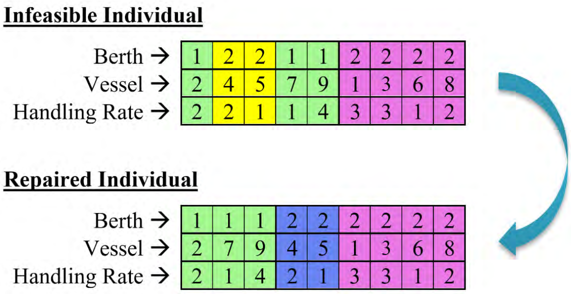

FIGURE 6. An example of a repairing operation.

P-4 Repairing Operation

$\boldsymbol{Repair}(Offspring_{gen})$
in: $Offspring_{gen}$- offspring produced by the mutation operator at generation gen
out: $\overline{Offspring_{gen}}$- repaired offspring at generation gen
1: $|\Phi| \leftarrow |Offspring_{gen}|$
2: $i \leftarrow 1$
3: **for all** $i \in Offspring_{gen}$ **do**
4: $\quad \Phi_i \leftarrow \boldsymbol{Sort}_{berth}(Offspring_{gen_i})$
5: $\quad i \leftarrow i + 1$
6: **end for**
7: $\overline{Offspring_{gen}} \leftarrow \Phi$
8: **return** $\overline{Offspring_{gen}}$

A temporary data structure for storing the repaired offspring chromosomes (Φ) is initialized in step 1. Then, the repairing operator starts an iterative process (steps 3-6), where for every offspring chromosome the gene arrays are sorted based on the assigned berth, and then the updated offspring chromosome is copied to the temporary data structure. The process continues until every infeasible individual is repaired. Next, the repairing operator replaces the infeasible offspring chromosomes with the repaired ones in step 7. Fig. 6 shows an example of a repairing operation, where the gene arrays with vessels "4" and "5" are shifted to the group of gene arrays that correspond to berth "2". The latter allows obtaining a feasible vessel service order at berth "1". The repairing operator is applied within the developed HEA to each infeasible offspring after deployment of the mutation operator.

F. FITNESS FUNCTION

The fitness function of the developed HEA algorithm was assumed to be equal to the objective function of the **GBSP** mathematical model (i.e., the total vessel service cost) without deployment of any additional scaling mechanisms [26].

G. SURVIVOR SELECTION

The survivor selection aims to identify the offspring chromosomes from the current population that will become candidate parents in the consecutive generation. This study applies a generational survivor selection mechanism, which assumes that all offspring chromosomes from the current population are allowed to become potential parents in the consecutive generation. The generational survivor selection mechanism has been widely deployed in canonical Genetic Algorithms and Genetic Programming [26].

H. TERMINATION CRITERION

The developed HEA algorithm will be terminated after a pre-specified number of generations (Gen_{Last}). The value of Gen_{Last} will be selected based on preliminary runs of the HEA algorithm, and details are presented in section V.B of the paper.

V. NUMERICAL EXPERIMENTS

A number of numerical experiments were conducted in this study to evaluate effectiveness of the proposed HEA algorithm and the developed berth scheduling model. The computational effectiveness of the developed HEA algorithm was assessed based on a comparative analysis against the following algorithms: 1) typical EA, which does not apply any local search heuristics; 2) hybrid EA, which applies only the GFCFS heuristic for the population initialization but does not apply the OHRS heuristic after the HEA operations (this algorithm will be referred to as HEA-1); and 3) hybrid EA, which applies only the OHRS heuristic after the HEA operations but does not apply the GFCFS heuristic for the population initialization (this algorithm will be referred to as HEA-2). All of the developed algorithms (i.e., EA, HEA-1, HEA-2, and HEA) were coded in MATLAB 2016a [28]. The numerical experiments were performed a Dell Intel(R) Core^{TM}i7 Processor with 32 GB of RAM. The **GBSP-R** mathematical model was coded in General Algebraic Modeling System - GAMS [29] and solved using CPLEX within the OHRS heuristic (used by the HEA-2 and HEA algorithms). This section of the paper provides a detailed description of the conducted numerical experiments, including the following major steps: 1) input data description; 2) parameter tuning analysis; 3) optimality gap estimation; 4) comprehensive comparison of the algorithms; and 5) analysis of the managerial insights.

A. INPUT DATA DESCRIPTION

The available MCT operations literature was primarily used to generate the numerical data for computational experiments in this study [30]–[39]. The adopted values for parameters of the **GBSP** mathematical model are presented in Table 1. A total of three MCT berthing availability cases were considered in this study, including the following: (1) 2 berths; (2) 4 berths; and (3) 6 berths. The interarrival time of vessels at the MCT was modeled using the exponential distribution with an average of 2 hours [32], [33]. The container demand for each vessel calling at the MCT was set as follows: $NC_v = U[500; 2{,}000] \forall v \in V$ (TEUs), where U – is a notation used to define the uniformly distributed pseudorandom numbers. It was assumed that the MCT operator could provide a total of four handling rates to the liner shipping companies. The

TABLE 1. Input data.

Parameter	Adopted Value
MCT berthing availability (berths)	[2; 4; 6]
Average vessel interarrival time (hours)	2
Container demand for each vessel: $NC_v, v \in V$ (TEUs)	$U[500; 2{,}000]$
Handling productivity at the "*preferred berth*": $hp_{vb_v^*h}, v \in V, b_v^* \in B, h \in H$ (TEUs/hour)	[120; 150; 180; 210]
Requested vessel departure: $RD_v, v \in V$ (hours)	$RD_v = AT_v + HT_v \cdot U[1.2; 1.4]$
CO_2 emission factor: $EF_{vbh}, v \in V, b \in B, h \in H$ (tons of CO_2/ TEU)	$EF_{vbh} = EF_{vbh^*} \cdot \frac{hp_{vbh}}{180} \cdot (1 + U[0.1; 0.2] \cdot \lvert b_v^* - b \rvert)$
Vessel handling cost: $c_{vh}^{HT}, v \in V, h \in H$ (USD/TEU)	$c_{vh}^{HT} = \frac{hp_{vb_v^*h}}{180} \cdot U[500; 750]$
Vessel waiting cost: $c_v^{WT}, v \in V$ (USD/hour)	$U[1{,}000; 2{,}000]$
Late departure penalty: $c_v^{LD}, v \in V$ (USD/hour)	$U[5{,}000; 10{,}000]$
CO_2 emission cost: c^{CO_2} (USD/ton)	32

handling productivities for corresponding handling rates at the "*preferred berth*" $hp_{vb_v^*h} \forall v \in V, b_v^* \in B, h \in H$ (where b_v^* – is the "*preferred berth*" for vessel v) were set to [120; 150; 180; 210] TEUs/hour respectively. The "*preferred berth*" for each vessel was determined based on the FCFS policy.

The handling productivity for vessel v at berth b under handling rate h was calculated as follows: $hp_{vbh} = hp_{vb_v^*h} \cdot (1 - U[0.1; 0.2] \cdot |b_v^* - b|) \forall v \in V, b, b_v^* \in B, h \in H$ (TEUs/hour). The latter formula accounts for decreasing productivity under the requested handling rate if a vessel is not scheduled for service at its "*preferred berth*" [21]. The requested vessel departure time was set based on the vessel arrival time and the vessel handling time (assuming that the vessel will be served at the "*preferred berth*").

Based on the available literature the CO_2 emission factor for the base handling productivity ($h^* = 180$ TEUs/hour) was set to $EF_{vbh^*} = 0.01729 \forall v \in V, b \in B, h^* \in H$ (tons of CO_2/TEU) [23], [24]. The CO_2 emission factors for handling rates with the other handling productivities were computed in relation to the base handling productivity as follows: $EF_{vbh} = EF_{vbh^*} \cdot \frac{hp_{vbh}}{180} \cdot (1 + U[0.1; 0.2] \cdot |b_v^* - b|) \forall v \in V, b, b_v^* \in B, h, h^* \in H$ (tons of CO_2/TEU). The latter formula allows capturing an increasing CO_2 emission production due to increasing handling productivity (i.e., the MCT operator will be required to deploy more handling equipment for service of a vessel, which will increase the CO_2 emissions produced) and/or additional container transfer time to the marshaling yard in case if a vessel is not scheduled for service at its "*preferred berth*" (i.e., additional container transfer time will increase the CO_2 emissions produced by the internal transport vehicles).

The vessel handling cost was set as follows: $c_{vh}^{HT} = \frac{hp_{vb_v^*h}}{180} \cdot U[500; 750] \forall v \in V, b_v^* \in B, h \in H$ (USD/TEU) [37]. The latter formula accounts for an increasing handling cost for requesting a handling rate with a higher handling productiv-

TABLE 2. Parameter tuning analysis summary.

Algorithm	Parameter	Parameter Description	Candidate Values	Selected Value
EA	$PopSize$	Population size	[20; 30; 40; 50]	50
EA	$CrosProb$	Crossover probability	[0.50; 0.60; 0.70; 0.80]	0.50
EA	$MutRate$	Mutation rate	[2; 4; 6; 8]	2
HEA-1	$PopSize$	Population size	[20; 30; 40; 50]	50
HEA-1	$CrosProb$	Crossover probability	[0.50; 0.60; 0.70; 0.80]	0.50
HEA-1	$MutRate$	Mutation rate	[2; 4; 6; 8]	2
HEA-2	$PopSize$	Population size	[20; 30; 40; 50]	40
HEA-2	$CrosProb$	Crossover probability	[0.50; 0.60; 0.70; 0.80]	0.50
HEA-2	$MutRate$	Mutation rate	[2; 4; 6; 8]	2
HEA-2	Ω	Subset of individuals selected for improvement (% of $PopSize$)	[5; 10; 20; 30]	10
HEA-2	Gen_{Ω}	Number of generations after each improvement	[50; 100; 200; 300]	50
HEA	$PopSize$	Population size	[20; 30; 40; 50]	40
HEA	$CrosProb$	Crossover probability	[0.50; 0.60; 0.70; 0.80]	0.50
HEA	$MutRate$	Mutation rate	[2; 4; 6; 8]	2
HEA	Ω	Subset of individuals selected for improvement (% of $PopSize$)	[5; 10; 20; 30]	10
HEA	Gen_{Ω}	Number of generations after each improvement	[50; 100; 200; 300]	50

ity. The vessel waiting and late departure costs were generated as follows: $c_v^{WT} = U[1{,}000; 2{,}000] \forall v \in V$ (USD/hour) and $c_v^{LD} = U[5{,}000; 10{,}000] \forall v \in V$ (USD/hour) [36]. The CO_2 emission cost was set to 32 (USD/ton) [23], [24]. A total of 60 problem instances were developed based on the generated numerical data by varying the number of vessels calling for service at MCT and the berthing availability at MCT. The generated problem instances were subdivided into the following groups: 1) small size problem instances (SP1-SP30) with the number of vessels changing from 11 to 20 with an increment of one vessel for each one of the berthing availability cases; 2) realistic size problem instances (RP1-RP30) with the number of vessels changing from 45 to 90 with an increment of five vessels for each one of the berthing availability cases. Results from the conducted computational experiments are reported in sections V.B-V.E of the paper.

B. PARAMETER TUNING

A parameter tuning analysis was conducted in this study to determine the values of parameters for each one of the developed solution algorithms. A factorial design methodology [40] was implemented for the parameter tuning analysis in this study. According to the factorial design methodology, each algorithm has a number of parameters, which are generally referred to as "*factors*", and each parameter has a set of candidate values, which are generally referred to as "*levels*". Five problem instances were selected at random from the developed large size problem instances (LP1-LP30), which were described in section V.A. Each algorithm was assumed to have four candidate values for each parameter (which corresponds to a 4^k factorial design with 4 levels and k factors). Each one of the developed algorithms was executed 10 times for each parameter combination. Hence, a total of $4^k \cdot repl \cdot inst$ experimental runs (where $repl$ – is the number of replications [$repl = 10$]; $inst$ – is the number of instances [$inst = 5$]) were undertaken for each one of the developed algorithms. The parameter tuning analysis results are presented in Table 2, where the following data are provided for each algorithm: (1) algorithm; (2) parameter of a given algorithm; (3) description of a given parameter; (4) considered candidate values; and (5) selected parameter value (based on a tradeoff between the solution quality at convergence and the recorded computational time).

Computational experiments also demonstrated that there was no substantial change in the objective function value after ~3,000 generations for each one of the algorithms. Therefore, the termination criterion was set to $Gen_{Last} = 3{,}000$ generations (for the EA, HEA-1, HEA-2, and HEA algorithms).

C. OPTIMALITY GAP ESTIMATION

The first set of numerical experiments aimed to estimate the optimality gaps for the developed solution algorithms in order to compare the objective function values, suggested by the algorithms, against the optimal ones. The **GBSP** mathematical model was coded in GAMS [29] and then solved using CPLEX for all the small size problem instances (SP1-SP30). The maximum allowable CPLEX computational time was limited to 2 hours, while 0.1% was adopted for the CPLEX relative optimality gap value. All of the developed algorithms were launched for the considered small size problem instances. The optimality gap analysis results are shown in Table 3, which provides the following information: (1) instance number; (2) number of vessels requesting service at MCT (i.e., $|V|$); (3) MCT berthing availability (i.e., $|B|$); (4) optimal objective function value, identified by CPLEX; (5) CPLEX computational time; (6) objective function values for the EA, HEA-1, HEA-2, and HEA algorithms (aver-

TABLE 3. Optimality gap analysis results.

Instance	$\|V\|$	$\|B\|$	CPLEX		EA			HEA-1			HEA-2			HEA		
			Objective, 10^6 USD	CPU, min	Objective, 10^6 USD	Optimality Gap, %	CPU, min	Objective, 10^6 USD	Optimality Gap, %	CPU, min	Objective, 10^6 USD	Optimality Gap, %	CPU, min	Objective, 10^6 USD	Optimality Gap, %	CPU, min
SP1	11	2	11.6384	0.041	11.6384	0.00	0.434	11.6384	0.00	0.456	11.6384	0.00	0.611	11.6384	0.00	0.666
SP2	11	4	10.8651	2.575	10.8651	0.00	0.450	10.8651	0.00	0.458	10.8651	0.00	0.640	10.8651	0.00	0.682
SP3	11	6	10.6310	8.250	10.6310	0.00	0.458	10.6310	0.00	0.465	10.6310	0.00	0.644	10.6310	0.00	0.695
SP4	12	2	12.9243	0.098	12.9243	0.00	0.459	12.9243	0.00	0.467	12.9243	0.00	0.631	12.9243	0.00	0.688
SP5	12	4	12.0010	5.857	12.0010	0.00	0.474	12.0010	0.00	0.478	12.0010	0.00	0.648	12.0010	0.00	0.704
SP6	12	6	11.7356	16.361	11.7356	0.00	0.485	11.7356	0.00	0.487	11.7356	0.00	0.662	11.7356	0.00	0.718
SP7	13	2	14.0499	0.134	14.0499	0.00	0.481	14.0499	0.00	0.490	14.0499	0.00	0.653	14.0499	0.00	0.711
SP8	13	4	13.0265	9.155	13.0265	0.00	0.496	13.0265	0.00	0.501	13.0265	0.00	0.670	13.0265	0.00	0.726
SP9	13	6	12.7226	24.666	12.7226	0.00	0.507	12.7226	0.00	0.511	12.7226	0.00	0.685	12.7226	0.00	0.742
SP10	14	2	14.8808	2.300	14.8808	0.00	0.507	14.8808	0.00	0.513	14.8808	0.00	0.674	14.8808	0.00	0.730
SP11	14	4	13.7581	16.801	13.7581	0.00	0.518	13.7581	0.00	0.521	13.7581	0.00	0.690	13.7581	0.00	0.742
SP12	14	6	13.4308	42.300	13.4308	0.00	0.530	13.4308	0.00	0.537	13.4308	0.00	0.705	13.4308	0.00	0.756
SP13	15	2	16.5775	7.999	16.5775	0.00	0.524	16.5775	0.00	0.531	16.5775	0.00	0.695	16.5775	0.00	0.747
SP14	15	4	15.2810	41.332	15.3526	0.47	0.526	15.2810	0.00	0.542	15.2810	0.00	0.712	15.2810	0.00	0.763
SP15	15	6	14.9109	58.265	15.1349	1.50	0.538	14.9109	0.00	0.551	14.9109	0.00	0.730	14.9109	0.00	0.780
SP16	16	2	17.8564	14.155	17.9837	0.71	0.536	17.8564	0.00	0.552	17.8564	0.00	0.715	17.8564	0.00	0.764
SP17	16	4	16.3049	53.634	16.5906	1.75	0.548	16.4667	0.99	0.561	16.4827	1.09	0.734	16.3849	0.49	0.784
SP18	16	6	15.7833	85.633	16.2138	2.73	0.561	15.9763	1.22	0.573	16.0423	1.64	0.772	15.9333	0.95	0.798
SP19	17	2	18.4843	24.666	18.7133	1.24	0.560	18.5929	0.59	0.578	18.6598	0.95	0.779	18.5443	0.32	0.791
SP20	17	4	16.8135	83.207	17.1983	2.29	0.574	17.0000	1.11	0.587	17.0276	1.27	0.748	16.9535	0.83	0.801
SP21	17	6	16.1877	119.485	16.8556	4.13	0.583	16.5709	2.37	0.599	16.6220	2.68	0.770	16.4477	1.61	0.817
SP22	18	2	19.8166	64.155	20.1550	1.71	0.582	19.9722	0.79	0.605	20.0711	1.28	0.755	19.9166	0.50	0.796
SP23	18	4	17.9058	112.818	18.3776	2.63	0.591	18.2513	1.93	0.606	18.2781	2.08	0.770	18.1658	1.45	0.816
SP24	18	6	N/A	>120	17.8904	N/A	0.602	17.7705	N/A	0.617	17.7922	N/A	0.792	17.6654	N/A	0.834
SP25	19	2	21.4556	104.485	21.9604	2.35	0.604	21.6515	0.91	0.619	21.7732	1.48	0.772	21.6356	0.84	0.818
SP26	19	4	N/A	>120	19.9252	N/A	0.613	19.7753	N/A	0.627	19.8085	N/A	0.790	19.6082	N/A	0.846
SP27	19	6	N/A	>120	19.3670	N/A	0.625	19.1762	N/A	0.636	19.2343	N/A	0.808	19.0253	N/A	0.856
SP28	20	2	N/A	>120	22.9932	N/A	0.622	22.7693	N/A	0.638	22.8219	N/A	0.785	22.4649	N/A	0.838
SP29	20	4	N/A	>120	20.6471	N/A	0.632	20.4557	N/A	0.646	20.5264	N/A	0.804	20.3265	N/A	0.860
SP30	20	6	N/A	>120	20.0260	N/A	0.644	19.8608	N/A	0.655	19.8932	N/A	0.826	19.6834	N/A	0.878

age over 10 replications); (7) optimality gap, estimated as $\Delta_i = (F_i - F^*)/F^*$, where F^*– is the optimal objective function value, identified by CPLEX; F_i – is the objective function value, identified by algorithm i ($i = EA, HEA-1, HEA-2, HEA$); and (8) computational time for the EA, HEA-1, HEA-2, and HEA algorithms (average over 10 replications).

Results from the optimality gap analysis showcase that for certain problem instances CPLEX was not able to obtain the optimal solution within 2 hours (i.e., instances SP24, SP26, SP27, SP28, SP29, and SP30). The latter finding can be explained by the *NP*-hard complexity of the **GBSP** mathematical model. The maximum optimality gap values comprised 4.13%, 2.37%, 2.68%, and 1.61% for the EA, HEA-1, HEA-2, and HEA algorithms respectively. The latter results demonstrate accuracy of the developed solution algorithms. Smaller optimality gaps were generally recorded for the HEA algorithm. The computational time, required to solve the small size problem instances, averaged on 32.53 sec, 33.22 sec, 43.34 sec, and 46.30 sec for the EA, HEA-1, HEA-2, and HEA algorithms respectively.

D. COMPREHENSIVE COMPARISON OF THE ALGORITHMS

The second set of numerical experiments focused on a comprehensive comparative analysis of the developed solution algorithms for the realistic size problem instances (RP1-RP30). Each one of the considered algorithms (i.e., EA, HEA-1, HEA-2, and HEA) was executed for all the generated realistic size problem instances, described in section V.A of the paper. Results of the conducted analysis are summarized in Table 4, including the following data: (1) instance number; (2) number of vessels requesting service at MCT (i.e., $|V|$); (3) MCT berthing availability (i.e., $|B|$); (4) the objective function value, identified by the GFCFS heuristic (i.e., starting solution for the HEA-1 and HEA algorithms); (5) objective function values for each algorithm (average over 10 replications); and (6) computational time values for each algorithm (average over 10 replications).

Computational experiments indicate that deployment of the GFCFS heuristic at the population initialization stage is more advantageous for the search process as compared to deployment of the OHRS heuristic after application of the crossover and mutation operators. The latter finding is supported by the fact that the HEA-1 algorithm suggests solutions with superior objective function values as opposed to the HEA-2 algorithm for all the generated realistic size problem instances.

Moreover, the developed HEA consistently outperforms the EA, HEA-1, and HEA-2 algorithms in terms of the objective function values. The objective function value, provided at convergence of the HEA algorithm, was on average 11.3%, 3.2%, and 7.7% lower as compared to the objective function values, suggested by the EA, HEA-1, and HEA-2 algorithms respectively. Hence, deployment of both GFCFS and OHRS heuristics (applied within the HEA algorithm) is more advantageous for exploration and exploitation of the promising domains of the search space as compared to deployment of either GFCFS only (applied within the HEA-1 algorithm) or OHRS only (applied within the HEA-2 algorithm). The worst performance was demonstrated by the EA algorithm, which solely relied on the stochastic search operators (i.e., crossover and mutation) without applying any local search. The computational time of the EA, HEA-1, HEA-2, and HEA algorithms averaged on 1.71 min, 1.73 min, 1.78 min, and 1.91 min respectively. Therefore, application of addi-

TABLE 4. Comparative analysis results.

Instance	$\|V\|$	$\|B\|$	GFCS	EA		HEA-1		HEA-2		HEA	
				Objective, 10^6 USD	CPU, min	Objective, 10^6 USD	CPU, min	Objective, 10^6 USD	CPU, min	Objective, 10^6 USD	CPU, min
RP1	45	2	83.5403	60.8332	1.207	58.2138	1.230	59.2860	1.305	56.4461	1.392
RP2	45	4	63.1346	49.0923	1.214	47.6143	1.234	48.4074	1.313	46.7664	1.406
RP3	45	6	56.7174	45.9873	1.221	45.0960	1.247	45.7233	1.335	44.3105	1.425
RP4	50	2	92.6056	67.2566	1.308	64.0502	1.333	65.8702	1.375	62.1514	1.449
RP5	50	4	68.4308	53.3904	1.313	51.6659	1.342	52.8748	1.417	50.6895	1.484
RP6	50	6	61.7658	50.1680	1.327	48.8274	1.358	49.4870	1.445	47.8804	1.519
RP7	55	2	103.0628	76.5448	1.427	71.7738	1.449	74.1930	1.482	69.1697	1.557
RP8	55	4	74.7927	58.8948	1.437	56.5104	1.460	58.0045	1.539	55.4020	1.943
RP9	55	6	68.1084	55.0738	1.447	53.3499	1.465	54.0119	1.561	52.3911	2.044
RP10	60	2	115.5349	85.3078	1.523	79.5207	1.556	82.1354	1.576	76.5132	1.715
RP11	60	4	81.4174	64.3295	1.541	61.0535	1.578	63.7618	1.626	59.8657	1.758
RP12	60	6	74.7699	59.7921	1.541	57.8596	1.579	59.0372	1.655	56.6439	1.787
RP13	65	2	127.0650	94.8382	1.637	87.8720	1.663	91.0515	1.690	83.5954	1.783
RP14	65	4	89.7116	70.0733	1.644	65.8085	1.672	68.7469	1.742	64.5407	1.811
RP15	65	6	82.3996	64.9159	1.655	62.3955	1.685	63.7806	1.761	61.0367	1.876
RP16	70	2	139.3056	104.7771	1.757	95.9870	1.786	99.8919	1.792	91.6484	1.908
RP17	70	4	97.7909	76.4301	1.778	70.7226	1.798	74.9078	1.850	69.3553	1.946
RP18	70	6	89.2895	70.7001	1.784	67.0426	1.797	69.1625	1.879	65.6541	1.989
RP19	75	2	151.7171	115.2194	1.871	104.2687	1.891	108.6774	1.889	99.1615	2.018
RP20	75	4	104.6765	82.7057	1.880	75.8322	1.913	80.8966	1.939	74.2387	2.070
RP21	75	6	99.0099	75.7881	1.879	72.0626	1.917	74.1971	1.968	70.2198	2.112
RP22	80	2	167.3425	125.0191	1.966	112.7645	2.003	118.2961	1.982	107.2708	2.119
RP23	80	4	113.5131	88.9085	1.982	80.5081	2.015	86.2316	2.046	78.8286	2.166
RP24	80	6	105.7297	80.7882	1.989	76.3788	2.023	79.3683	2.078	74.4575	2.221
RP25	85	2	179.1998	134.4596	2.073	119.1757	2.112	126.7009	2.105	113.4176	2.223
RP26	85	4	119.8380	93.4197	2.083	83.8030	2.115	90.3281	2.162	82.0808	2.276
RP27	85	6	110.2138	85.6984	2.104	79.5716	2.116	83.3621	2.197	77.6153	2.323
RP28	90	2	192.1391	145.6273	2.187	128.5982	2.218	136.3589	2.222	121.6071	2.318
RP29	90	4	127.7450	100.7245	2.198	88.6017	2.219	97.5649	2.287	86.9014	2.371
RP30	90	6	117.3808	90.6461	2.219	84.2862	2.224	88.1555	2.314	82.0845	2.434

tional local search heuristics within the HEA-1, HEA-2, and HEA algorithms did not substantially influence their time complexity.

Along with the objective function and computational time values, the algorithmic convergence patterns were recorded for each problem instance and each replication. Results are illustrated in Fig. 7 for the first replication of each algorithm for problem instances RP19-RP30 (i.e., 12 out of 30 problem instances with the largest size). The convergence patterns are shown only for the first replication, as they did not fluctuate substantially from one replication to another for each one of the developed solution algorithms. The convergence pattern analysis results indicate that the random population initialization (applied within the EA and HEA-2 algorithms) drastically worsens the quality of the initial solutions. On the other hand, deployment of the GFCFS heuristic (applied within the HEA-1 and HEA algorithms) allows the search to begin within the promising domains, which have solutions with higher fitness values. Furthermore, application of the ORHS heuristic allows refining solutions produced by the stochastic search operators, which further allows HEA discovering solutions with higher fitness function values as compared to HEA-1 throughout the search process.

E. ANALYSIS OF THE MANAGERIAL INSIGHTS

The third set of numerical experiments was conducted to demonstrate how the developed mathematical model could be used to draw important managerial insights. A total of 220 scenarios were developed by changing the CO_2 emission cost from 32 USD/ton (base case) to 640 USD/ton with an increment of 32 USD/ton and increasing the late arrival penalty from 100% (base case) to 200% with an increment of 10% for each vessel calling at the MCT. The analysis was performed for the problem instance with the largest size (RP30). The HEA algorithm was executed for each one of the CO_2 emission cost - late vessel arrival penalty scenarios. Results are presented in Fig. 8, where the following information is provided for each scenario: (1) total vessel service cost; (2) total vessel late departures; and (3) total CO_2 emissions produced due to container handling. Note that the average vessel late arrival penalty was estimated as follows: $\overline{c^{LD}} = (\sum_{v \in V} c_v^{LD})/|V|$.

It can be observed that a simultaneous increase of the CO_2 emission cost and the late vessel arrival penalties may increase the total vessel service cost by 1.93 million USD as compared to the base case total vessel service cost (for $CO_2 = 32$ USD/ton and $\overline{c^{LD}} = 7{,}640$ USD/hour).

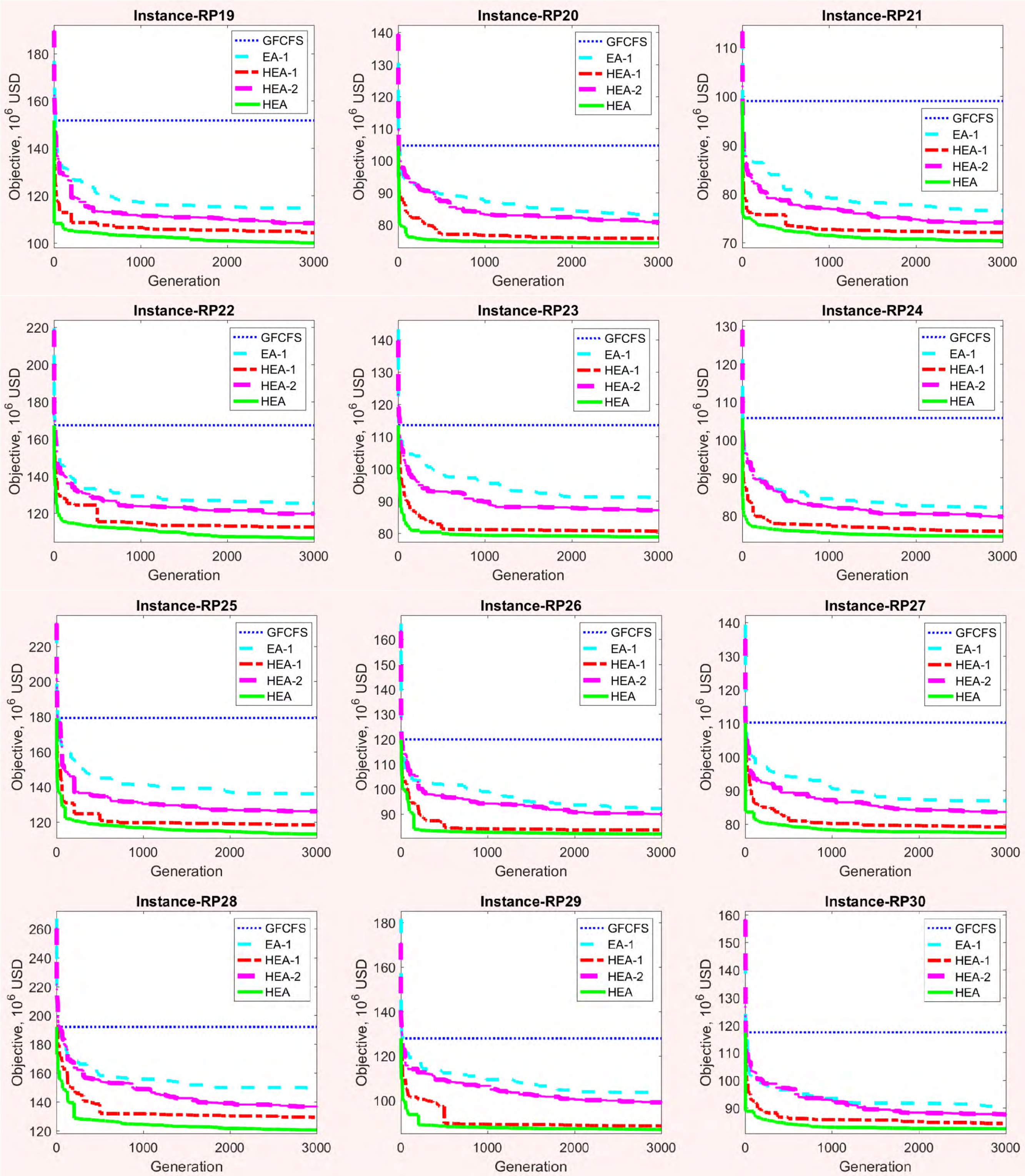

FIGURE 7. Convergence patterns of the developed algorithms.

Furthermore, an increase in the average vessel late departure penalty from 7,640 USD/hour to 15,300 USD/hour reduced the total vessel late arrival hours from 47.1 hours to 34.8 hours for the base case CO_2 emission cost value ($CO_2 =$ 32 USD/ton). In the meantime, an increase in the CO_2 emission cost from 32 USD/ton to 640 USD/ton reduced

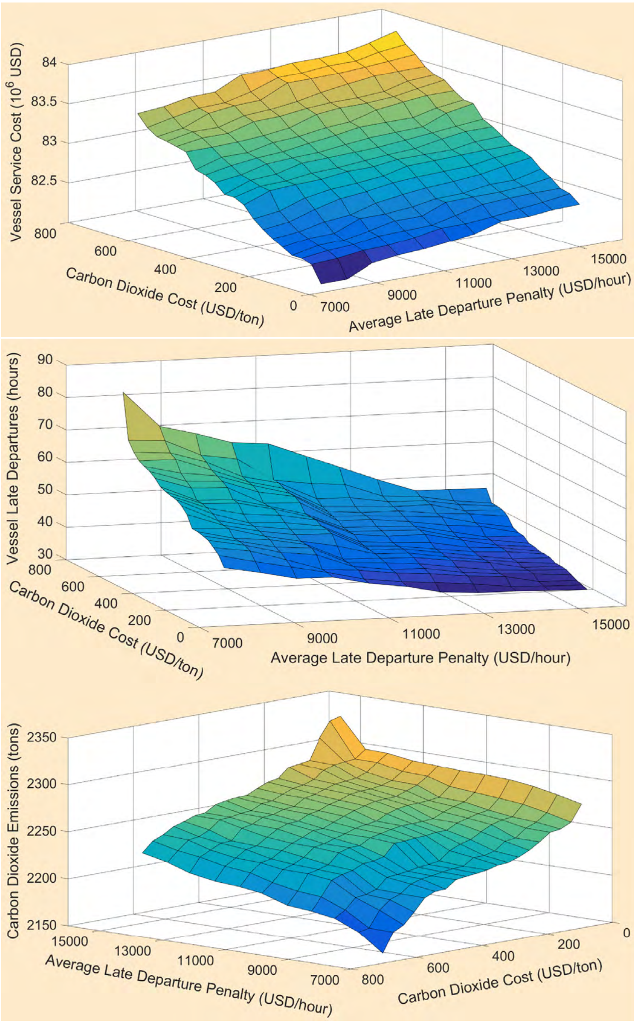

FIGURE 8. Managerial insights.

the total CO_2 emission production from 2,274.1 tons to 2,153.4 tons for the base case average vessel late arrival penalty value ($\overline{c^{LD}} = 7{,}640$ USD/hour). Hence, the developed mathematical model can assist the MCT operator with construction of efficient berth schedules, improving the environmental sustainability of the MCT operations, evaluation of various CO_2 taxation polices, and analysis of various agreements with the liner shipping companies (i.e., how the MCT operator should alter the berth schedule if the liner shipping company increases costs associated with vessel late departures, waiting time, etc.).

VI. CONCLUSIONS AND FUTURE RESEARCH EXTENSIONS

Considering a substantial increase in the international seaborne trade volumes, the marine container terminal operators have to enhance effectiveness of the operations in order to handle the growing demand. In the meantime, negative environmental externalities have to be accounted for in management of the terminal operations. This study proposed a mixed integer mathematical model for the berth scheduling problem, where the objective function minimized the total vessel service cost, including the carbon dioxide emission cost due to container handling. Due to the *NP*-hard complexity of the presented mathematical model the Hybrid Evolutionary Algorithm was developed to solve the realistic size problem instances within an acceptable computational time. Unlike typical stochastic search algorithms, the proposed algorithm deployed a set of local search heuristics to facilitate exploration and exploitation of the search space. Results for the conducted numerical experiments indicated that the optimality gap of the developed Hybrid Evolutionary Algorithm did not exceed 1.61%. Moreover, application of local search heuristics allowed the proposed solution algorithm an efficient discovering of good quality solutions without a substantial increase in the computational time. The analysis of managerial insights indicated that the carbon dioxide emission cost might significantly affect the design of berth schedules. Therefore, the presented mathematical model and the developed solution approach may assist the marine container terminal operators with designing the cost-effective berth schedules and improving the environmental sustainability of the terminal operations.

The avenues for the future research include the following: (1) application of the exact optimization algorithms within the proposed Green First Come First Served heuristic at the chromosome initialization stage; (2) deployment of the alternative crossover operators (e.g., partially mapped crossover); (3) application of the alternative survivor selection mechanism; (4) evaluation of new termination criteria for the solution algorithm; (5) application of scaling mechanisms for the fitness function; (6) evaluation of the alternative container handling equipment types and their effects on the environmental sustainability of the terminal operations; and (7) modeling the other pollutants, produced by container handling equipment.

REFERENCES

[1] *Review of Maritime Transport 2016*, United Nations Conf. Trade Develop., Geneva, Switzerland, 2016.

[2] L. Chen *et al.*, "Container port performance measurement and comparison leveraging ship GPS traces and maritime open data," *IEEE Trans. Intell. Transp. Syst.*, vol. 17, no. 5, pp. 1227–1242, Dec. 2015.

[3] J. Polcari, "An informative interpretation of decision theory: Scalar performance measures for binary decisions," *IEEE Access*, vol. 2, pp. 1456–1480, Dec. 2014.

[4] R. Li, H. Harai, and H. Asaeda, "An aggregatable name-based routing for energy-efficient data sharing in big data era," *IEEE Access*, vol. 3, pp. 955–966, Jun. 2015.

[5] J. Wu, I. Akingeneye, and J. Yang, "Energy efficient optimum sensing with energy harvesting power sources," *IEEE Access*, vol. 3, pp. 989–997, Jul. 2015.

[6] T. M. Nguyen, V. N. Ha, and L. B. Le, "Resource allocation optimization in multi-user multi-cell massive MIMO networks considering pilot contamination," *IEEE Access*, vol. 3, pp. 1272–1287, Aug. 2015.

[7] M. M. Golias, G. K. Saharidis, M. Boile, S. Theofanis, and M. G. Ierapetritou, "The berth allocation problem: Optimizing vessel arrival time," *Maritime Econ. Logistics*, vol. 11, no. 4, pp. 358–377, Nov. 2009.

[8] J. F. Alvarez, T. Longva, and E. S. Engebrethsen, "A methodology to assess vessel berthing and speed optimization policies," *Maritime Econ. Logistics*, vol. 12, no. 4, pp. 327–346, Nov. 2010.

[9] S. Esmemr, I. B. Ceti, and O. Tuna, "A simulation for optimum terminal truck number in a Turkish port based on lean and green concept," *Asian J. Shipping Logistics*, vol. 26, no. 2, pp. 277–296, Dec. 2010.
[10] M. Golias, M. Boile, S. Theofanis, and C. Efstathiou, "The berth-scheduling problem: Maximizing berth productivity and minimizing fuel consumption and emissions production," *Transp. Res. Rec., J. Transp. Res. Board*, vol. 2166, pp. 208–227, Oct. 2010.
[11] N. Lang and A. Veenstra, "A quantitative analysis of container vessel arrival planning strategies," *OR Spectr.*, vol. 32, no. 3, pp. 477–499, Jul. 2010.
[12] Y. Du, Q. Chen, X. Quan, L. Long, and R. Y. K. Fung, "Berth allocation considering fuel consumption and vessel emissions," *Transp. Res. E, Logistics Transp. Rev.*, vol. 47, no. 6, pp. 1021–1037, Nov. 2011.
[13] S. Wang, Q. Meng, and Z. Liu, "A note on 'Berth allocation considering fuel consumption and vessel emissions,"' *Transp. Res. E, Logistics Transp. Rev.*, vol. 49, no. 1, pp. 48–54, Jan. 2013.
[14] G. Chen, K. Govindan, and M. M. Golias, "Reducing truck emissions at container terminals in a low carbon economy: Proposal of a queueing-based bi-objective model for optimizing truck arrival pattern," *Transp. Res. E, Logistics Transp. Rev.*, vol. 55, pp. 3–22, Aug. 2013.
[15] D. Chang, Z. Jiang, W. Yan, and J. He, "Integrating berth allocation and quay crane assignments," *Transp. Res. E, Logistics Transp. Rev.*, vol. 46, no. 6, pp. 975–990, Nov. 2010.
[16] J. He, W. Zhang, Y. Huang, and W. Yan, "A simulation optimization method for internal trucks sharing assignment among multiple container terminals," *Adv. Eng. Inform.*, vol. 27, no. 4, pp. 598–614, Oct. 2013.
[17] J. He, Y. Huang, and W. Yan, "Yard crane scheduling in a container terminal for the trade-off between efficiency and energy consumption," *Adv. Eng. Inform.*, vol. 29, no. 1, pp. 59–75, Jan. 2015.
[18] J. He, Y. Huang, W. Yan, and S. Wang, "Integrated internal truck, yard crane and quay crane scheduling in a container terminal considering energy consumption," *Expert Syst. Appl.*, vol. 42, no. 5, pp. 2464–2487, Apr. 2015.
[19] EPA. (Nov. 2016). *Causes of Climate Change*. [Online]. Available: https://www3.epa.gov/climatechange/science/causes.html
[20] Live Science. (Dec. 2016). *Global Warming: News, Facts, Causes & Effects*. [Online]. Available: http://www.livescience.com/topics/global-warming
[21] C. Bierwirth and F. Meisel, "A follow-up survey of berth allocation and quay crane scheduling problems in container terminals," *Eur. J. Oper. Res.*, vol. 244, no. 3, pp. 675–689, Dec. 2014.
[22] M. A. Dulebenets, "Models and solution algorithms for improving operations in marine transportation," Ph.D. Dissertation, Dept. Civil Eng., Univ. Memphis, Memphis, TN, USA, 2015.
[23] N. K. Tran, H.-D. Haasis, and T. Buer, "Container shipping route design incorporating the costs of shipping, inland/feeder transport, inventory and CO_2 emission," *Maritime Econ. Logistics*, pp. 1–28, Mar. 2016. [Online]. Available: http://link.springer.com/article/10.1057/mel.2016.11
[24] A. Schroten, H. van Essen, and R. Anthes, "External cost calculator—Methodology report," CE Delft, Delft, The Netherlands, Tech. Rep. 11.4212.67, Sep. 2011. [Online]. Available: http://ecocalc-test.ecotransit.org/methodology_report.pdf
[25] M. L. Pinedo, *Scheduling: Theory, Algorithms, and Systems*. Springer, 2008. [Online]. Available: http://www.springer.com/in/book/9781489990433
[26] A. E. Eiben and J. E. Smith, *Introduction to Evolutionary Computing*. Springer, 2003. [Online]. Available: http://www.springer.com/us/book/9783642072857
[27] A. Imai, E. Nishimura, and S. Papadimitriou, "Berthing ships at a multi-user container terminal with a limited quay capacity," *Transp. Res. E, Logistics Transp. Rev.*, vol. 44, no. 1, pp. 136–151, Jan. 2008.
[28] Mathworks. (Mar. 2014). *Release 2014a*. [Online]. Available: http://www.mathworks.com/products/matlab/whatsnew.html
[29] GAMS. (Jan. 2017). *GAMS Home Page*. [Online]. Available: https://www.gams.com/
[30] M. A. Dulebenets, E. E. Ozguven, R. Moses, and M. B. Ulak, "Intermodal freight network design for transport of perishable products," *Open J. Optim.*, vol. 5, no. 4, pp. 120–139, Dec. 2016.
[31] M. A. Dulebenets, "Bunker consumption optimization in liner shipping: A metaheuristic approach," *Int. J. Recent Innov. Trends Comput. Commun.*, vol. 3, no. 6, pp. 3766–3776, Jun. 2015.
[32] A. Imai, E. Nishimura, M. Hattori, and S. Papadimitriou, "Berth allocation at indented berths for mega-containerships," *Eur. J. Oper. Res.*, vol. 179, no. 2, pp. 579–593, Jun. 2007.
[33] A. Imai, E. Nishimura, and S. Papadimitriou, "Marine container terminal configurations for efficient handling of mega-containerships," *Transp. Res. E, Logistics Transp. Rev.*, vol. 49, no. 1, pp. 141–158, Jan. 2013.
[34] M. A. Dulebenets, "Advantages and disadvantages from enforcing emission restrictions within emission control areas," *Maritime Bus. Rev.*, vol. 1, no. 2, pp. 107–132, Dec. 2016.
[35] M. A. Dulebenets, "A new simulation model for a comprehensive evaluation of yard truck deployment strategies at marine container terminals," *Open Sci. J.*, vol. 1, no. 3, pp. 1–23, Oct. 2016.
[36] S. Zampelli, Y. Vergados, R. Van Schaeren, W. Dullaert, and B. Raa, "The berth allocation and quay crane assignment problem using a CP approach," in *Principles and Practice of Constraint Programming*, vol. 8124. Springer, 2013, pp. 880–896. [Online]. Available: http://link.springer.com/chapter/10.1007/978-3-642-40627-0_64
[37] The Port Authority of New York and New Jersey. (Jan. 2017). *Marine Terminal Tariffs*. [Online]. Available: http://www.panynj.gov/port/tariffs.html
[38] M. A. Dulebenets, "The vessel scheduling problem in a liner shipping route with heterogeneous fleet," *Int. J. Civil Eng.*, pp. 1–14, Oct. 2016. [Online]. Available: http://link.springer.com/article/10.1007/s40999-016-0060-z
[39] M. A. Dulebenets and E. E. Ozguven, "Vessel scheduling in liner shipping: Modeling transport of perishable assets," *Int. J. Prod. Econ.*, vol. 184, pp. 141–156, Feb. 2017.
[40] E. B. de Lima, G. L. Pappa, J. M. de Almeida, M. A. Gonçalves, and W. Meira, "Tuning genetic programming parameters with factorial designs," in *Proc. IEEE Congr. Evol. Comput.*, Barcelona, Spain, Jul. 2010, pp. 1–8.

MAXIM A. DULEBENETS received the B.S. and M.Sc. degrees in railway construction from the Moscow State University of Railroad Engineering, Moscow, Russia, and the M.Sc. and Ph.D. degrees in civil engineering from the University of Memphis, Memphis, TN, USA, with concentration in transportation. He is currently an Assistant Professor with the Department of Civil and Environmental Engineering, Florida A&M University-Florida State University. His research interests include but are not limited to operations research, optimization, simulation modeling, *NP*-hard problems, evolutionary computation, metaheuristics, mathematical programming, hybrid algorithms, transportation engineering, liner shipping scheduling, and GPS data processing. He is an invited Young Member of the Standing Committee on Ports and Channels (AW010) of the Transportation Research Board of the National Academy of Sciences, USA. He is a licensed Professional Engineer registered in the State of Michigan.

REN MOSES is currently a Professor with the Department of Civil and Environmental Engineering, Florida A&M University-Florida State University. He has conducted and managed projects related to highway safety, traffic operations, ITS, and development of workforce in the highway construction industry. He is active nationally in the Transportation Research Board and the Institute of Transportation Engineering. He has authored over 100 publications in national and international transportation-related refereed journals and conference proceedings. He has supervised over 20 Ph.D. and M.Sc. students with theses and dissertations on safety and operations of multimodal systems.

EREN E. OZGUVEN received the B.S. degree in civil engineering and the M.Sc. degree in industrial engineering from the Bogazici University, Istanbul, Turkey, the Ph.D. degree in civil and environmental engineering from the Rutgers University, New Brunswick, NJ, USA, with concentration in emergency supply transportation operations. He is currently an Assistant Professor with the Department of Civil and Environmental Engineering, Florida A&M University-Florida State University. His research interests include smart cities, urban mobility, traffic safety and reliability, emergency transportation, and intelligent transportation systems.

ARDA VANLI received the B.S. degree in mechanical engineering from the Middle East Technical University, Ankara, Turkey, in 1998, the M.S. degree in mechanical engineering from the Pennsylvania State University in 2000, and the Ph.D. degree in industrial engineering and operations research from Pennsylvania State University, in 2007. He joined the Florida State University in 2008. He is currently an Associate Professor with the Department of Industrial and Manufacturing Engineering, Florida A&M University-Florida State University. His research focuses on monitoring, control, and optimization of manufacturing processes, condition monitoring and reliability modeling of engineering systems, and calibration and validation of computational models. His research is published in peer-reviewed journals, including *Technometrics*, *IIE Transactions*, IEEE TRANSACTIONS ON SEMICONDUCTOR MANUFACTURING, *Quality and Reliability Engineering International*, and *Mechanical Systems and Signal Processing*.